JOURNAL OF MEDICINAL FOOD
J Med Food 17 (6) 2014, 641–649

DOI: 10.1089/jmf.2013.2965

Effects of Curcumin (*Curcuma longa*) on Learning and Spatial Memory as Well as Cell Proliferation and Neuroblast Differentiation in Adult and Aged Mice by Upregulating Brain-Derived Neurotrophic Factor and CREB Signaling

Sung Min Nam,[1,*] Jung Hoon Choi,[2,*] Dae Young Yoo,[1] Woosuk Kim,[1] Hyo Young Jung,[1] Jong Whi Kim,[1] Miyoung Yoo,[3] Sanghee Lee,[3] Chul Jung Kim,[4] Yeo Sung Yoon,[1] and In Koo Hwang[1]

[1]*Department of Anatomy and Cell Biology, College of Veterinary Medicine, and Research Institute for Veterinary Science, Seoul National University, Seoul, South Korea.*
[2]*Department of Anatomy, College of Veterinary Medicine, Kangwon National University, Chuncheon, South Korea.*
[3]*Food Analysis Center, Korea Food Research Institute, Sungnam, South Korea.*
[4]*Natural Pond Co., Ltd., Seoul, South Korea.*

ABSTRACT Aging is a progressive process, and it may lead to the initiation of neurological diseases. In this study, we investigated the effects of wild Indian *Curcuma longa* using a Morris water maze paradigm on learning and spatial memory in adult and D-galactose-induced aged mice. In addition, the effects on cell proliferation and neuroblast differentiation were assessed by immunohistochemistry for Ki67 and doublecortin (DCX) respectively. The aging model in mice was induced through the subcutaneous administration of D-galactose (100 mg/kg) for 10 weeks. *C. longa* (300 mg/kg) or its vehicle (physiological saline) was administered orally to adult and D-galactose-treated mice for the last three weeks before sacrifice. The administration of *C. longa* significantly shortened the escape latency in both adult and D-galactose-induced aged mice and significantly ameliorated D-galactose-induced reduction of cell proliferation and neuroblast differentiation in the subgranular zone of hippocampal dentate gyrus. In addition, the administration of *C. longa* significantly increased the levels of phosphorylated CREB and brain-derived neurotrophic factor in the subgranular zone of dentate gyrus. These results indicate that *C. longa* mitigates D-galactose-induced cognitive impairment, associated with decreased cell proliferation and neuroblast differentiation, by activating CREB signaling in the hippocampal dentate gyrus.

KEY WORDS: • ***brain-derived neurotrophic factor*** • ***CREB*** • **Curcuma longa** • ***D-galactose*** • ***subgranular zone***

INTRODUCTION

AGING IS PART OF THE NATURAL LIFE CYCLE of an organism and is associated with various morphological, functional, and biochemical changes in the body. Recently, the average human life-span has increased due to improvements in the quality of medical treatments and public health. One of the major phenotypes caused by aging is cognitive impairments, as well as the decreased neurogenesis in the hippocampus.[1,2] Chronic administration of a low dose of D-galactose (D-gal) results in similar characteristics to natural aging in animals.[3] D-gal is a reducing sugar, which is normally metabolized when consumed at typical levels in animals. However, an oversupply of D-gal is not metabolized normally[4] and leads to the accumulation of galactitol in the cell, resulting in osmotic stress and the production of reactive oxygen species (ROS).[5]

There have been numerous attempts to overcome age-related memory impairment and to reduce the ROS in the brain. Some medical plants have the potential to attenuate memory deficits in artificial and natural aging models.[6–9] One of these medicinal plants, *Curcuma longa*, has well-established neuroprotective effects in the brain against ischemic damage,[10–12] Alzheimer's disease,[13–15] Parkinson's disease,[16,17] and parathion-induced damage.[18] *C. longa* extract contains a polyphenolic nonflavonon compound—curcumin—which is a pharmacologically active substance.[19] Although curcumin has poor bioavailability,[20,21] it has been reported that it is a very effective agent in brain disease models such as amygdaloid kindled seizures in rats,[22] an iron-induced experimental model of epileptogenesis,[23] and electroshock seizures in mice[24] because it can cross the blood–brain barrier to enter brain tissue in spite of its poor bioavailability. Curcumin has been concentrated

*Sung Min Nam and Jung Hoon Choi contributed equally to this article.

Manuscript received 13 June 2013. Revision accepted 25 February 2014.

Address correspondence to: In Koo Hwang, DVM, PhD, Department of Anatomy and Cell Biology, College of Veterinary Medicine, Seoul National University, Seoul 151-742, South Korea, E-mail: vetmed2@snu.ac.kr

chiefly in the hippocampus in the kinetics of tissue distribution.[25] It has been reported that oral administration of curcumin improves learning and memory in aged rats[26,27] and mice,[28] and that it is protective against chronic unpredictable stress-induced cognitive impairment and associated oxidative damage in mice.[29]

The hippocampus region of the brains plays an important role in memory formation and spatial navigation. There is increasing evidence supporting the view that adult hippocampal neurogenesis is closely related to pattern separation and spatial memory.[30,31] Progenitor cells located in the subgranular zone of the hippocampal dentate gyrus divide, proliferate, differentiate, and give rise to new neurons.[32] Although several studies have found an overall age-related decline in cell proliferation,[33–39] there are few reports identifying factors that promote neurogenesis in the dentate gyrus of aged mice. Improvement in the microenvironment of neural stem cells in the subgranular zone of dentate gyrus, including ROS elimination and neurotrophic factor restoration, may be a promising strategy for enhancing successful aging. In this study, we examined the effects of *C. longa* using a Morris water maze paradigm on learning and spatial memory, as well as cell proliferation and neuroblast differentiation, in adult and D-gal-induced aged mice.

MATERIALS AND METHODS

Preparation of wild Indian C. longa

Rhizomes of *C. longa* were provided by Natural Pond Co., Ltd. (Seoul, South Korea). They were cleaned, dried, chopped, and blended using a Waring blender (1-L laboratory blender, 8010S; Waring Laboratory Science, Torrington, CT). The blended powder was left to soak in 95% ethanol at a ratio of 1:10 of plant to ethanol for three days at room temperature with shaking. The mixture was then filtered, and the resulting liquid was concentrated under a vacuum at 45°C in an EYELA rotary evaporator (N-1001S-W; EYELA USA, Bohemia, NY, USA) to yield a dark gummy-yellow extract (7.4%, w/w). The concentrated extract was then kept in an incubator at 45°C for 5 days to evaporate the ethanol residue, yielding the crude rhizome extract. Extracts were kept at room temperature with silica gel until used. Extracts were dissolved in 10% Tween-20 before being orally administrated to animals, and the insoluble materials were removed through centrifugation (1000 *g*) at room temperature.

Experimental animals

Male C57BL/6 mice were purchased from Japan SLC, Inc. (Shizuoka, Japan), and housed under in a controlled environment maintaining temperature (23°C) and humidity (60%) and a 12/12 h light/dark cycle, and free access to food and tap water. The handling and caring of the animals conformed to published guidelines (NIH Guide for the Care and Use of Laboratory Animals, NIH Publication No. 85-23, 1985, revised 1996), and were approved by the Institutional Animal Care and Use Committee (IACUC) of Seoul National University (SNU-110511-6). Every effort was made to minimize the number of animals used and the suffering caused by the procedures.

Administration of drugs and C. longa

The animals were divided into four groups ($n = 10$ per group): vehicle (10% Tween-20), 300 mg/kg *C. longa* extract (C300), D-gal (100 mg/kg; Sigma, St. Louis, MO, USA), and D-gal with C300 (D-gal + C300; Fig. 1). D-gal was subcutaneously administered to six-week-old mice once a day for 10 weeks. At 13 weeks of age, vehicle or C300 was orally administered to mice once a day for three weeks. The different experimental groups ran individually in time. The dosage of *C. longa* was chosen because oral administration of *C. longa* significantly decreases lipid peroxidation and increases antioxidants activity.[40] These schedules were adopted because doublecortin (DCX; a marker for neuroblasts) is exclusively expressed in immature neurons from 1 to 28 days of cell age.[41,42]

Water maze performance

At the 10th week after D-gal administration, spatial memory was assayed using Morris water maze tests as previously reported.[43,44] The behavioral test and sacrifice of animals were conducted at 9:00–11:00 a.m. At three days after the training, the time required for an individual mouse to find the submerged platform within two minutes (escape latency) and the swimming distance were monitored by a digital camera and a computer system for four consecutive days and four trials per day. The administration of D-gal and/or C300 was continued during the water maze performance. For each trial, a mouse was placed in the water facing the wall at one of four starting positions and released. The swimming speed and the time required for the mouse to find the hidden platform were recorded via a visual tracking system. The probe test was done on day 5; the platform was removed and the time that a mouse spent swimming in the target quadrant and in the three nontarget quadrants (right, left, and opposite quadrants) was measured, and the number of times the mouse crossed over the platform site was recorded.

Tissue processing for histology

For histology, on the day after the water maze test, animals in the vehicle-, C300, D-gal-, and D-gal + C300-treated groups ($n = 5$ in each group) were randomly selected and

FIG. 1. Experimental protocol in this study. *D-gal treatment (100mg/kg, S.C.) (black line) for 10 weeks; #Vehicle and C300 (300 mg/kg) treatment (green dot) for 3 weeks; †Water maze test (red dot) for 1 week. Color images available online at www.liebertpub.com/jmf

were anesthetized with 30 mg/kg Zoletil 50® (Virbac, Carros, France) at 09:00–11:00 a.m. to avoid the interference of the stress hormone. The animals were perfused transcardially with 0.1 M phosphate-buffered saline (PBS; pH 7.4) followed by 4% paraformaldehyde in 0.1 M phosphate buffer (PB; pH 7.4). The brains were removed and postfixed in the same fixative for four hours. The brain tissues were dehydrated with graded concentrations of alcohol for embedding in paraffin. Sections 3 μm thick were serially cut using a microtome (Leica, RM2245; Leica Biosystems, Newcastle upon Tyne, United Kingdom), and they were mounted onto silane-coated slides.

Immunohistochemistry

In order to obtain accurate data, immunohistochemical staining was carefully conducted under the same conditions. Tissue sections were selected between 1.96 and 2.26 mm posterior to the bregma in reference to a mouse atlas for each animal.[45] The sections were placed in 400 mL jars filled with citrate buffer (pH 6.0) and heated in a microwave oven (Optiquick Compact, Moulinex, Ecully Cedex, France) operating at a frequency of 2.45 GHz on a 800 W power setting. After three heating cycles of five minutes each, slides were allowed to cool at room temperature and were washed in PBS. They were next incubated with rabbit anti-Ki67 (a marker for cell proliferation) antibody (1:1000; Abcam, Cambridge, United Kingdom), goat anti-DCX antibody (1:50; Santa Cruz Biotechnology, Santa Cruz, CA, USA), rabbit anti-pCREB (phosphorylated CREB, diluted 1:1000, Millipore, Temecula, CA, USA), or rabbit anti-BDNF (brain-derived neurotrophic factor, 1:1000; Chemicon International, Temecula, CA, USA) overnight, and subsequently exposed to biotinylated rabbit antigoat, or goat antirabbit IgG (diluted 1:200; Vector, Burlingame, CA, USA) and streptavidin peroxidase complex (diluted 1:200, Vector). Then, the sections were visualized by reaction with 3,3′-diaminobenzidine tetrahydrochloride (Sigma).

Measurements of Ki67-, DCX-, or pCREB-immunoreactive cells in all the groups were performed using an image analysis system equipped with a computer-based CCD camera (Olympus, DP71, Tokyo, Japan; software: Optimas 6.5, CyberMetrics, Scottsdale, AZ, USA). The Ki67-, DCX-, or pCREB-immunoreactive cells in each section of the dentate gyrus were counted using Optimas 6.5 software. The cell counts from all of the sections of all of the mice were averaged.

Measurement of BDNF levels

To confirm the effects of C300 and/or D-gal on BDNF levels, the remaining animals in each group ($n = 5$) were sacrificed under anesthesia (Zoletil 50®) by decapitation on the day after the water maze test (9:00–11:00 a.m.), and hippocampal dentate gyri were dissected out using the Pix-Cell II system (Arcturus Engineering, Mountain View, CA, USA). BDNF levels were measured with a Promega BDNF Emax immunoassay kit (Madison, WI, USA). Briefly, samples were weighed and 300 μL lysis buffer was added to each sample. Samples were sonicated for 30 sec and centrifuged (16,000 *g*) at 4°C for 20 min. The supernatant was stored at −20°C until analysis. All samples were assayed in duplicate, and absorbance was read on an enzyme-linked immunosorbant assay (ELISA) plate reader (Bio-Tek, Winooski, VT, USA). The concentration of each sample was calculated by a computer by plotting the absorbance values on a standard curve with known concentrations generated by the assay.

Statistical analysis

The data presented represent the means of the experiments performed for each experimental investigation. The differences among the means were statistically analyzed by a two-way analysis of variance followed by a Bonferroni's *post-hoc* method in order to elucidate the differences (D-gal × C300). $P < .05$ was considered statistically significant.

RESULTS

Effects of D-gal and/or C300 on spatial memory

In the vehicle-treated group, the mean escape latency was decreased within one day after initiation of the trials. In the C300-treated group, the mean escape latency was slightly shorter than in the vehicle-treated group throughout each day of the trial. However, no significant difference was observed in latency times between the vehicle- and C300-treated groups. In the D-gal-treated group, the escape latency was significantly longer during each day of the trial compared to that in the vehicle-treated group. In the D-gal + C300-treated group, the escape latency was significantly shorter throughout each day of the trial compared to that in the D-gal-treated group. However, it was longer during each day of the trial compared to that reported for the vehicle-treated group (Fig. 2A).

The mean swimming speed in the C300-treated group was slightly faster than that in the vehicle-treated group, but in the D-gal-treated group, swimming speed was significantly slower than that in the vehicle-treated group. In the D-gal + C300-treated group, the swimming speed was significantly increased compared to that in the D-gal-treated group (Fig. 2B).

The platform crossings in the probe trial were similar between vehicle- and C300-treated groups. In the D-gal-treated group, there were significantly fewer platform crossings in the probe trial compared to the vehicle-treated group. In the D-gal + C300-treated group, the frequency of crossing over the platform site increased compared to that in the D-gal-treated group (Fig. 2C).

Spatial preference for the target quadrant was similar between vehicle- and D-gal-treated groups. Spatial preference was significantly decreased in the D-gal-treated group compared to that in the vehicle-treated group. In the D-gal + C300-treated group, spatial preference was significantly increased compared to that in the D-gal-treated group (Fig. 2D).

Effects of D-gal and/or C300 on cell proliferation

In each group, Ki67-immunoreactive nuclei were detected in the subgranular zone of the dentate gyrus. However,

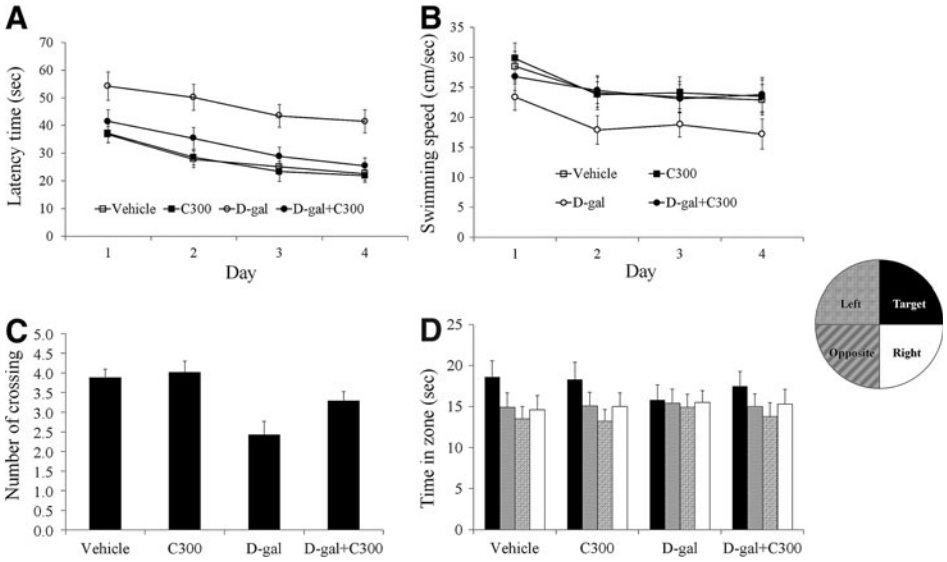

FIG. 2. Spatial memory test using a Morris water maze in the vehicle-, C300-, D-gal-, and D-gal + C300-treated groups ($n = 10$ per group). **(A)** Mean latency time in the hidden platform test. **(B)** Swimming speeds in the hidden platform test. **(C)** The number of crossings over the exact location of the former platform. **(D)** Comparison of time spent in the target quadrant with other quadrants on day 5. Error bar indicates standard error of the mean (SEM).

there were significant differences in the numbers of Ki67-immunorecactive nuclei between treatment groups. In the vehicle-treated group, the average number of Ki67-immunoreactive nuclei was 7.7 per section (Fig. 3A, E). In the C300-treated group, the mean number of Ki67-immunoreactive nuclei was significantly increased compared to the vehicle-treated group with 9.9 per section (Fig. 3B, E). In the D-gal-treated group, Ki67-immunoreactive nuclei were not clustered, and the average number of Ki67-immunoreactive nuclei was significantly decreased compared to those of the vehicle-treated group with 2.9 per section (Fig. 3C, E). In the D-gal + C300-treated group, the mean number of Ki67-immunoreactive nuclei was significantly increased compared to that in the D-gal-treated group and was 5.7 per section (Fig. 3D, E). However, the mean number of Ki67-positive nuclei in this group was less than that reported for the vehicle-treated group (Fig. 3D, E).

Effects of D-gal and/or C300 on neuroblast differentiation

In each group, the soma of DCX-immunoreactive neuroblasts was observed in the subgranular zone of the dentate gyrus with dendrites extending into the molecular layer of dentate gyrus. However, there were significant differences in the number of DCX-immunoreactive neuroblasts with dendrites between the groups. In the vehicle-treated group, the average number of DCX-immunoreactive neuroblasts was 32.5 per section (Fig. 4A, B, I). In the C300-treated group, DCX-immunoreactive neuroblasts with dendrites were abundant compared to those in the vehicle-treated group. In this group, the average number of DCX-immunoreactive neuroblasts was 52.1 per section (Fig. 4C, D, I). In the D-gal-treated group, the average number of DCX-immunoreactive neuroblasts was significantly decreased compared to the vehicle-treated group with 12.6 per section (Fig. 4E, F, I). In the D-gal + C300-treated group, the mean number of DCX-immunoreactive neuroblasts was significantly increased compared to the D-gal-treated group with 30.1 per section (Fig. 4G–I). The mean number of DCX-immunoreactive neuroblasts was similar to that reported for the vehicle-treated group. However, there were fewer dendrites observed in the DCX-positive neuroblasts compared to the vehicle-treated group (Fig. 4I).

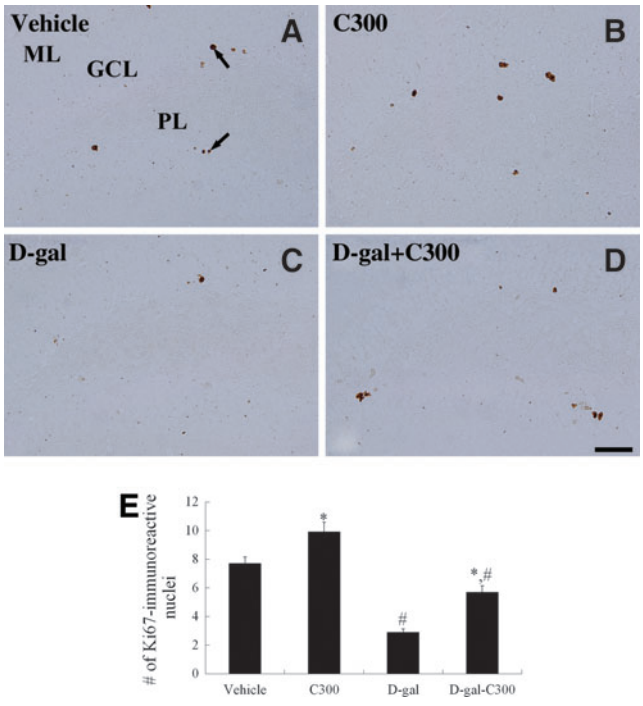

FIG. 3. Immunohistochemistry for Ki67 in the dentate gyrus of the **(A)** vehicle-, **(B)** C300-, **(C)** D-gal-, and **(D)** D-gal + C300-treated groups. Scale bar = 50 μm. **(E)** The mean number of Ki67-positive cells per section in all groups ($n = 5$ per group; $^{*}P < .05$, indicating a significant difference between vehicle/D-gal and C300/D-gal + C300; $^{\#}P < .05$, a significant difference between vehicle/C300 and D-gal/D-gal + C300). Error bar indicates SEM. GCL, granule cell layer; ML, molecular layer; PL, polymorphic layer. Color images available online at www.liebertpub.com/jmf

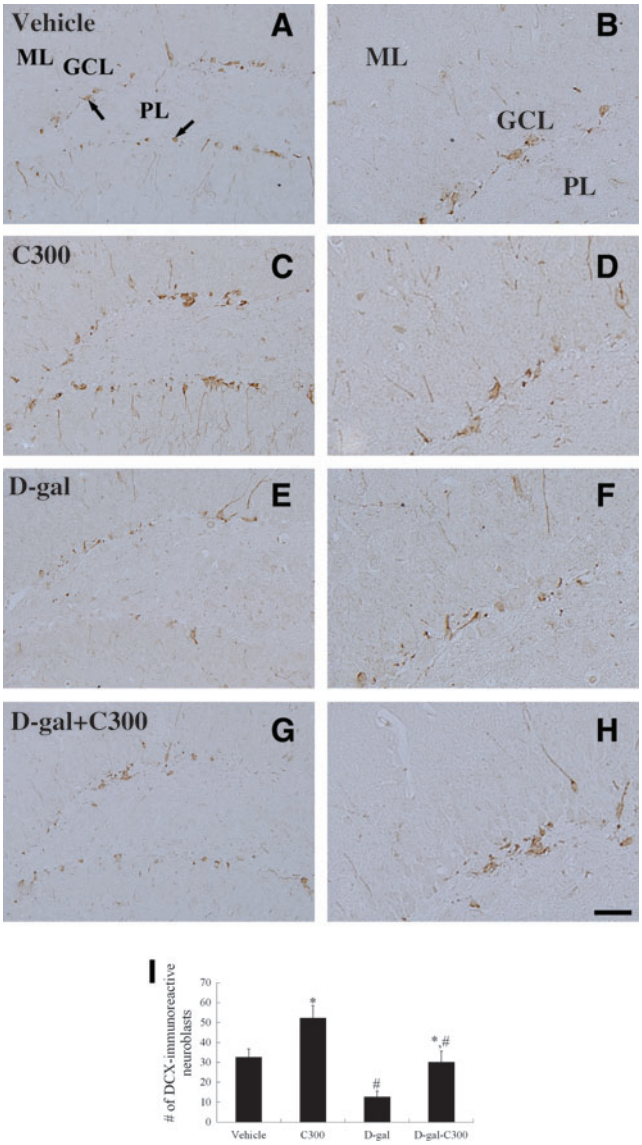

FIG. 4. Immunohistochemistry for doublecortin (DCX) in the dentate gyrus of **(A, B)** vehicle-, **(C, D)** C300-, **(E, F)** D-gal-, and **(G, H)** D-gal + C300-treated groups. Scale bar = 50 μm **(A, C, E, G)**; 25 μm **(B, D, F, H)**. **(I)** The mean number of DCX-immunoreactive neuroblasts per section in all groups ($n = 5$ per group; $^{*}P < .05$, indicating a significant difference between vehicle/D-gal and C300/D-gal + C300; $^{\#}P < .05$, a significant difference between vehicle/C300 and D-gal/D-gal + C300). Error bar indicates SEM. Color images available online at www.liebertpub.com/jmf

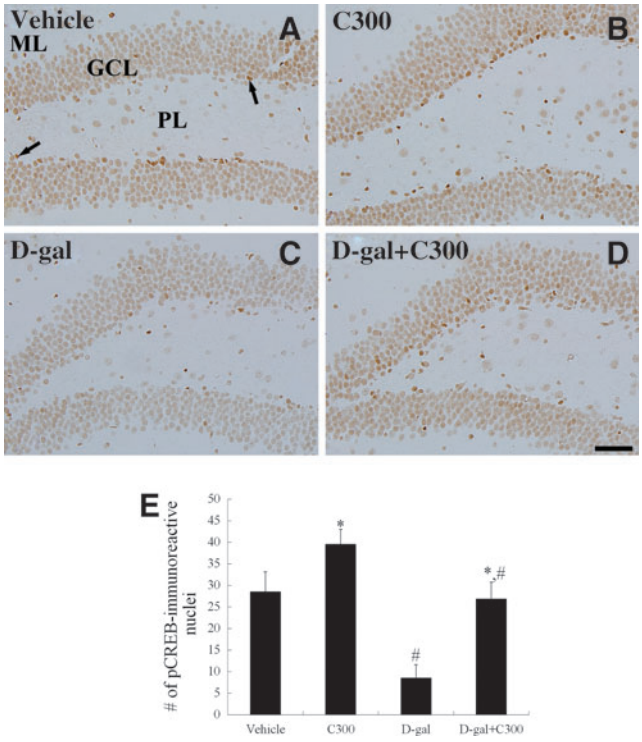

FIG. 5. Immunohistochemistry for phosphorylated CREB (pCREB) in the dentate gyrus of **(A)** vehicle-, **(B)** C300-, **(C)** D-gal-, and **(D)** D-gal + C300- treated groups. Scale bar = 50 μm. **(E)** The mean number of pCREB-immunoreactive nuclei per section in all groups ($n = 5$ per group; $^{*}P < .05$, indicating a significant difference between vehicle/D-gal and C300/D-gal + C300; $^{\#}P < .05$, a significant difference between vehicle/C300 and D-gal/D-gal + C300). Error bar indicates SEM. Color images available online at www.liebertpub.com/jmf

Effects of D-gal and/or C300 on phosphorylation of CREB

In each treatment group, the pCREB-immunoreactive nuclei were mainly detected in the subgranular zone of the dentate gyrus. The average number of pCREB-immunoreactive nuclei was significantly different among the groups. In the vehicle-treated group, the average number of the pCREB-immunoreactive nuclei was 28.5 per section (Fig. 5A, E). In the C300-treated group, the average number of pCREB-immunoreactive nuclei increased compared to the vehicle-treated group with 39.5 per section (Fig. 5B, E). In the D-gal-treated group, pCREB-immunoreactive nuclei were significantly decreased compared to the vehicle-treated group. In this group, the average number of pCREB-immunoreactive nuclei quantitated was 8.5 per section (Fig. 5C, E). In the D-gal + C300-treated group, the average number of pCREB-immunoreactive nuclei was significantly increased compared to the D-gal-treated group with 26.8 per section (Fig. 5D, E).

Effects of D-gal and/or C300 on BDNF immunoreactivity and protein levels

In the vehicle-treated group, BDNF immunoreactivity was detected in a few cells in the dentate gyrus (Fig. 6A). In this group, the mean BDNF protein level in the dentate gyrus homogenates was 86.5 pg/mg (Fig. 6E). In the C300-treated group, BDNF immunoreactivity was prominently observed in the dentate gyrus (Fig. 6B), and the average BDNF protein level was reported as 128.4 pg/mg protein (Fig. 6E). In the D-gal-treated group, BDNF immunoreactivity was almost undetectable in the dentate gyrus (Fig. 6C), and the average BDNF protein level was markedly decreased (41.8 pg/mg) when compared to that in the vehicle-treated group (Fig. 6E). In the D-gal + C300-treated group, BDNF immunoreactivity was detected in the dentate gyrus

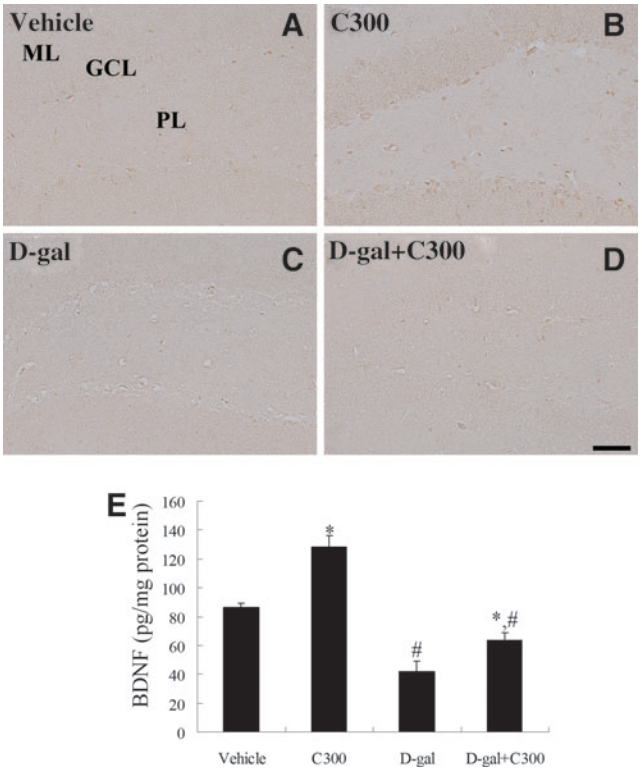

FIG. 6. Immunohistochemistry for brain-derived neurotrophic factor (BDNF) in the dentate gyrus of **(A)** vehicle-, **(B)** C300-, **(C)** D-gal-, and **(D)** D-gal + C300-treated groups. Scale bar = 50 μm. **(E)** Levels of BDNF in vehicle-, C300-, D-gal-, and D-gal + C300-treated groups ($n = 5$ per group; $^{*}P < .05$, indicating a significant difference between vehicle/D-gal and C300/D-gal + C300; $^{\#}P < .05$, a significant difference between vehicle/C300 and D-gal/D-gal + C300). Error bar indicates SEM. Color images available online at www.liebertpub.com/jmf

(Fig. 6D), and the mean BDNF levels were significantly higher than that in the D-gal-treated group, but the BDNF protein level was significantly decreased (63.3 pg/mg) compared to that of the vehicle-treated group (Fig. 6E).

DISCUSSION

Chronic systemic exposure to D-gal in mice gives rise to the acceleration of senescence and includes shortened life-span,[3] cognitive deficits,[46] increased ROS, and suppressed antioxidant enzyme activity.[2,3] In the present study, we found that curcumin extract protected against memory impairment in the D-gal induced aged mice. The administration of C300 ameliorated the D-gal-induced increased latency times and decreased swimming speed, platform crossings, and spatial preference for the target quadrant compared to those reported in the counterpart control mice. This result is supported by previous studies that have shown that *C. longa* extract significantly ameliorates memory deficits in D-gal-induced senescence mice,[28] prevents decreases in acetylcholinesterase activity in aged rats[26,27] and mice with Alzheimer's disease[47] and chronic unpredictable stress condition.[29] It has reported that the protective effect of curcumin on memory deficit is mediated by prevention of oxidative stress. Chronic curcumin oral treatment significantly improved the colchicine-induced cognitive impairment in mice by decreasing lipid peroxidation.[48,49] In addition, curcumin reversed ethanol-induced memory deficit via suppression of nitric oxide synthase/nitric oxide pathway.[50] Curcumin shows neuroprotective effects against ethanol-, aluminum-, and iron-induced neurotoxicity in rodents.[51,52] In the okadaic acid-induced impairment model, oral administration of curcumin significantly improves the memory function as assessed by both Morris water maze and passive avoidance tests.[53] Under normal aging and increased oxidative stress conditions, memory function declines due to decreases in BDNF.[54,55] On the other hand, enhanced BDNF improved learning and memory impairments.[56,57] It has been reported that BDNF is closely related to learning and memory by directly examining its role in a variety of learning paradigms in rodents.[58,59] In the present study, we found that C300 administration enhanced BDNF expression in the hippocampus (Fig. 7). This result may suggest that enhanced BDNF expression by curcumin may prevent memory impairment induced by the D-gal aging model.

Numerous studies have reported that aging decreases the proliferation of progenitor cells in the dentate gyrus of the hippocampus.[2,33–39] In this study, we confirmed that the administration of D-gal significantly decreased cell proliferation and neuroblast differentiation as seen in the aging process. The administration of C300 significantly increased cell proliferation and neuroblast differentiation in adult mice. It has been reported that the administration of curcumin significantly increases embryonic neural stem cell viability and proliferation.[60] In the D-gal-induced aging model, C300 significantly mitigated the D-gal-induced decrease in cell proliferation and neuroblast differentiation. It has been reported that curcumin ameliorates the stress-induced impairment of neurogenesis in rats.[61] However, the detailed mechanism involved in the enhanced neurogenesis observed by the treatment with curcumin remains unknown.

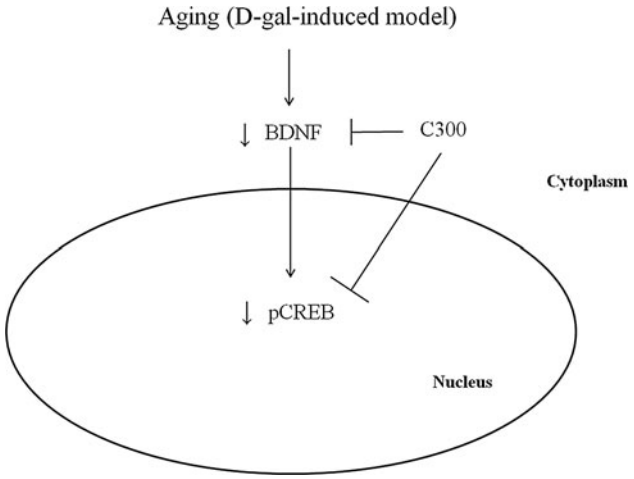

FIG. 7. A proposed mechanistic diagram of C300 action in this study.

It has been reported that curcumin can reverse the decreased levels of monoamines, including serotonin, noradrenalin, and dopamine, in the rat brain due to olfactory bulbectomy[62] and exposure to conditions of stress.[63–65] Activation of serotonin receptors coupled to cAMP production and CREB activation can induce transcription of the BDNF gene.[66] BDNF plays a central role in brain development and plasticity by opposing neuronal damage and promoting neurogenesis and cell survival.[67,68] BDNF-tyrosine kinase B signaling leads to phosphorylation and activation of transcription factors such as CREB, which induces gene expression and long-lasting synaptic changes.[69,70] In the present study, we observed that the administration of C300 significantly increased BDNF immunoreactivity and protein levels in the dentate gyrus. In addition, the administration of C300 significantly increased pCREB immunoreactivity in the dentate gyrus of adult and aging mice. This result is supported by a previous study demonstrating that the administration of curcumin increases hippocampal neurogenesis in chronically stressed rats via upregulation of the 5-HT_{1A} receptor and BDNF in the hippocampus.[61] In addition, curcumin protects neurons from chronic stress, depression, and glutamate excitotoxicity by activating BDNF levels.[71–75] In a depression-like model induced by olfactory bulbectomy, curcumin significantly ameliorated the hyperactivity in an open field test as well as reducing BDNF levels in the whole brain.[76]

In conclusion, the present study indicates that the administration of C300 mitigates D-gal-induced memory impairment, as well as the reduction of cell proliferation and neuroblast differentiation, through the activation of CREB and BDNF in the dentate gyrus.

ACKNOWLEDGMENTS

This work was supported by Basic Science Research Program through the National Research Foundation of Korea (NRF) funded by the Ministry of Science, ICT and Future Planning (2011-0013933).

AUTHOR DISCLOSURE STATEMENT

No competing financial interests exist.

REFERENCES

1. Bizon JL, Lee HJ, Gallagher M: Neurogenesis in a rat model of age-related cognitive decline. *Aging Cell* 2004;3:227–234.
2. Zhang Q, Li X, Cui X, Zuo P: D-galactose injured neurogenesis in the hippocampus of adult mice. *Neurol Res* 2005;27:552–556.
3. Cui X, Wang L, Zuo P, Han Z, Fang Z, Li W, Liu J: D-galactose-caused life shortening in *Drosophila melanogaster* and *Musca domestica* is associated with oxidative stress. *Biogerontology* 2004;5:317–325.
4. Kaplan LA, Pesce AJ: *Clinical Chemistry*. 3rd ed. Mosby, St. Louis, MO, USA, 1996.
5. Hsieh HM, Wu WM, Hu ML: Soy isoflavones attenuate oxidative stress and improve parameters related to aging and Alzheimer's disease in C57BL/6J mice treated with D-galactose. *Food Chem Toxicol* 2009;47:625–632.
6. Shi C, Xiao S, Liu J, Guo K, Wu F, Yew DT, Xu J: *Ginkgo biloba* extract EGb761 protects against aging-associated mitochondrial dysfunction in platelets and hippocampi of SAMP8 mice. *Platelets* 2010;21:373–379.
7. Jeong K, Shin YC, Park S, Park JS, Kim N, Um JY, Go H, Sun S, Lee S, Park W, Choi Y, Song Y, Kim G, Jeon C, Park J, Lee K, Bang O, Ko SG: Ethanol extract of *Scutellaria baicalensis* Georgi prevents oxidative damage and neuroinflammation and memorial impairments in artificial senescence mice. *J Biomed Sci* 2011;18:14.
8. Liu Y, Aisa HA, Ji C, Yang N, Zhu H, Zuo P: Effects of *Gossypium herbaceam* extract administration on the learning and memory function in the naturally aged rats: neuronal niche improvement. *J Alzheimers Dis* 2012;31:101–111.
9. Prisila Dulcy C, Singh HK, Preethi J, Rajan KE: Standardized extract of *Bacopa monniera* (BESEB CDRI-08) attenuates contextual associative learning deficits in the aging rat's brain induced by D-galactose. *J Neurosci Res* 2012;90:2053–2064.
10. Jiang J, Wang W, Sun YJ, Hu M, Li F, Zhu DY: Neuroprotective effect of curcumin on focal cerebral ischemic rats by preventing blood–brain barrier damage. *Eur J Pharmacol* 2007;561:54–62.
11. Dohare P, Garg P, Sharma U, Jagannathan NR, Ray M: Neuroprotective efficacy and therapeutic window of curcuma oil: in rat embolic stroke model. *BMC Complement Altern Med* 2008;8:55.
12. Rathore P, Dohare P, Varma S, Ray A, Sharma U, Jagannathan NR, Ray M: Curcuma oil: reduces early accumulation of oxidative product and is anti-apoptogenic in transient focal ischemia in rat brain. *Neurochem Res* 2008;33:1672–1682.
13. Frautschy SA, Hu W, Kim P, Miller SA, Chu T, Harris-White ME, Cole GM: Phenolic anti-inflammatory antioxidant reversal of Aβ-induced cognitive deficits and neuropathology. *Neurobiol Aging* 2001;22:993–1005.
14. Yang F, Lim GP, Begum AN, Ubeda OJ, Simmons MR, Ambegaokar SS, Chen PP, Kayed R, Glabe CG, Frautschy SA, Cole GM: Curcumin inhibits formation of amyloid β oligomers and fibrils, binds plaques, and reduces amyloid *in vivo*. *J Biol Chem* 2005;280:5892–5901.
15. Garcia-Alloza M, Borrelli LA, Rozkalne A, Hyman BT, Bacskai BJ: Curcumin labels amyloid pathology *in vivo*, disrupts existing plaques, and partially restores distorted neurites in an Alzheimer mouse model. *J Neurochem* 2007;102:1095–1104.
16. Mansouri Z, Sabetkasaei M, Moradi F, Masoudnia F, Ataie A: Curcumin has neuroprotection effect on homocysteine rat model of Parkinson. *J Mol Neurosci* 2012;47:234–242.
17. Jiang TF, Zhang YJ, Zhou HY, Wang HM, Tian LP, Liu J, Ding JQ, Chen SD: Curcumin ameliorates the neurodegenerative pathology in A53T α-synuclein cell model of Parkinson's disease through the downregulation of mTOR/p70S6K signaling and the recovery of macroautophagy. *J Neuroimmune Pharmacol* 2013;8:356–369.
18. Canales-Aguirre AA, Gomez-Pinedo UA, Luquin S, Ramírez-Herrera MA, Mendoza-Magaña ML, Feria-Velasco A: Curcumin protects against the oxidative damage induced by the pesticide parathion in the hippocampus of the rat brain. *Nutr Neurosci* 2012;15:62–69.
19. Ganguli M, Chandra V, Kamboh MI, Johnston JM, Dodge HH, Thelma BK, Juyal RC, Pandav R, Belle SH, DeKosky ST: Apolipoprotein E polymorphism and Alzheimer disease: the Indo-US Cross-National Dementia Study. *Arch Neurol* 2000;57:824–830.

20. Sharma RA, Gescher AJ, Steward WP: Curcumin: the story so far. *Eur J Cancer* 2005;41:1955–1968.
21. Anand P, Kunnumakkara AB, Newman RA, Aggarwal BB: Bioavailability of curcumin: problems and promises. *Mol Pharm* 2007;4:807–818.
22. Du P, Li X, Lin HJ, Peng WF, Liu JY, Ma Y, Fan W, Wang X: Curcumin inhibits amygdaloid kindled seizures in rats. *Chin Med J (Engl)* 2009;122:1435–1438.
23. Jyoti A, Sethi P, Sharma D: Curcumin protects against electrobehavioral progression of seizures in the iron-induced experimental model of epileptogenesis. *Epilepsy Behav* 2009;14:300–308.
24. Bharal N, Sahaya K, Jain S, Mediratta PK, Sharma KK: Curcumin has anticonvulsant activity on increasing current electroshock seizures in mice. *Phytother Res* 2008;22:1660–1664.
25. Tsai YM, Chien CF, Lin LC, Tsai TH: Curcumin and its nanoformulation: the kinetics of tissue distribution and blood–brain barrier penetration. *Int J Pharm* 2011;416:331–338.
26. Conboy L, Foley AG, O'Boyle NM, Lawlor M, Gallagher HC, Murphy KJ, Regan CM: Curcumin-induced degradation of PKCδ is associated with enhanced dentate NCAM PSA expression and spatial learning in adult and aged Wistar rats. *Biochem Pharmacol* 2009;77:1254–1265.
27. Pyrzanowska J, Piechal A, Blecharz-Klin K, Lehner M, Skórzewska A, Turzyńska D, Sobolewska A, Plaznik A, Widy-Tyszkiewicz E: The influence of the long-term administration of *Curcuma longa* extract on learning and spatial memory as well as the concentration of brain neurotransmitters and level of plasma corticosterone in aged rats. *Pharmacol Biochem Behav* 2010;95:351–358.
28. Kumar A, Prakash A, Dogra S: Protective effect of curcumin (*Curcuma longa*) against D-galactose-induced senescence in mice. *J Asian Nat Prod Res* 2011;13:42–55.
29. Rinwa P, Kumar A: Piperine potentiates the protective effects of curcumin against chronic unpredictable stress-induced cognitive impairment and oxidative damage in mice. *Brain Res* 2012;1488:38–50.
30. Sahay A, Scobie KN, Hill AS, O'Carroll CM, Kheirbek MA, Burghardt NS, Fenton AA, Dranovsky A, Hen R: Increasing adult hippocampal neurogenesis is sufficient to improve pattern separation. *Nature* 2011;472:466–470.
31. Stone SS, Teixeira CM, Devito LM, Zaslavsky K, Josselyn SA, Lozano AM, Frankland PW: Stimulation of entorhinal cortex promotes adult neurogenesis and facilitates spatial memory. *J Neurosci* 2011;31:13469–13484.
32. Duman RS: Depression: a case of neuronal life and death? *Biol Psychiatry* 2004;56:140–145.
33. Kuhn HG, Dickinson-Anson H, Gage FH: Neurogenesis in the dentate gyrus of the adult rat: age-related decrease of neuronal progenitor proliferation. *J Neurosci* 1996;16:2027–2033.
34. Kempermann G, Kuhn HG, Gage FH: Experience-induced neurogenesis in the senescent dentate gyrus. *J Neurosci* 1998;18:3206–3212.
35. Cameron HA, McKay RD: Restoring production of hippocampal neurons in old age. *Nat Neurosci* 1999;2:894–897.
36. Molofsky AV, Slutsky SG, Joseph NM, He S, Pardal R, Krishnamurthy J, Sharpless NE, Morrison SJ: Increasing p16INK4a expression decreases forebrain progenitors and neurogenesis during ageing. *Nature* 2006;443:448–452.
37. Hwang IK, Yoo KY, Yi SS, Kwon YG, Ahn YK, Seong JK, Lee IS, Yoon YS, Won MH: Age-related differentiation in newly generated DCX immunoreactive neurons in the subgranular zone of the gerbil dentate gyrus. *Neurochem Res* 2008;33:867–872.
38. Hwang IK, Yoo KY, Park OK, Choi JH, Lee CH, Won MH: Comparison of density and morphology of neuroblasts in the dentate gyrus among variously aged dogs, German shepherds. *J Vet Med Sci* 2009;71:211–215.
39. Choi JH, Yoo KY, Lee CH, Park OK, Yan BC, Li H, Hwang IK, Park JH, Kim SK, Won MH: Comparison of newly generated doublecortin-immunoreactive neuronal progenitors in the main olfactory bulb among variously aged gerbils. *Neurochem Res* 2010;35:1599–1608.
40. Ali Hussain HEM: Hypoglycemic, hypolipidemic and antioxidant properties of combination of curcumin from *Curcuma longa*, Linn, and partially purified product from *Abroma augusta*, Linn. in streptozotocin induced diabetes. *Indian J Clin Biochem* 2002;17:33–43.
41. Brown JP, Couillard-Després S, Cooper-Kuhn CM, Winkler J, Aigner L, Kuhn HG: Transient expression of doublecortin during adult neurogenesis. *J Comp Neurol* 2003;467:1–10.
42. Couillard-Despres S, Winner B, Schaubeck S, Aigner R, Vroemen M, Weidner N, Bogdahn U, Winkler J, Kuhn HG, Aigner L: Doulecortin expression levels in adult brain reflect neurogenesis. *Eur J Neurosci* 2005;21:1–14.
43. Yoo DY, Kim W, Kim IH, Nam SM, Chung JY, Choi JH, Yoon YS, Won MH, Hwang IK: Combination effects of sodium butyrate and pyridoxine treatment on cell proliferation and neuroblast differentiation in the dentate gyrus of D-galactose-induced aging model mice. *Neurochem Res* 2012;37:223–231.
44. Yoo DY, Kim W, Lee CH, Shin BN, Nam SM, Choi JH, Won MH, Yoon YS, Hwang IK: Melatonin improves D-galactose-induced aging effects on behavior, neurogenesis, and lipid peroxidation in the mouse dentate gyrus via increasing pCREB expression. *J Pineal Res* 2012;52:21–28.
45. Franklin KBJ, Paxinos G: *The Mouse Brain in Stereotaxic Coordinates*. 2nd ed. Academic Press, San Diego, CA, USA, 1997.
46. Deng HB, Cui DP, Jiang JM, Feng YC, Cai NS, Li DD: Inhibiting effects of *Achyranthes bidentata* polysaccharide and *Lycium barbarum* polysaccharide on nonenzyme glycation in D-galactose induced mouse aging model. *Biomed Environ Sci* 2003;16:267–275.
47. Pan R, Qiu S, Lu DX, Dong J: Curcumin improves learning and memory ability and its neuroprotective mechanism in mice. *Chin Med J (Engl)* 2008;121:832–839.
48. Kumar A, Naidu PS, Seghal N, Padi SS: Effect of curcumin on intracerebroventricular colchicine-induced cognitive impairment and oxidative stress in rats. *J Med Food* 2007;10:486–494.
49. Kumar P, Padi SS, Naidu PS, Kumar A: Possible neuroprotective mechanisms of curcumin in attenuating 3-nitropropionic acid-induced neurotoxicity. *Methods Find Exp Clin Pharmacol* 2007;29:19–25.
50. Yu SY, Zhang M, Luo J, Zhang L, Shao Y, Li G: Curcumin ameliorates memory deficits via neuronal nitric oxide synthase in aged mice. *Prog Neuropsychopharmacol Biol Psychiatry* 2013;45C:47–53.
51. Kumar A, Dogra S, Prakash A: Protective effect of curcumin (*Curcuma longa*), against aluminium toxicity: possible behavioral and biochemical alterations in rats. *Behav Brain Res* 2009;205:384–390.
52. Yu SY, Gao R, Zhang L, Luo J, Jiang H, Wang S: Curcumin ameliorates ethanol-induced memory deficits and enhanced brain

nitric oxide synthase activity in mice. *Prog Neuropsychopharmacol Biol Psychiatry* 2013;44C:210–216.
53. Rajasekar N, Dwivedi S, Tota SK, Kamat PK, Hanif K, Nath C, Shukla R: Neuroprotective effect of curcumin on okadaic acid induced memory impairment in mice. *Eur J Pharmacol* 2013; 715:381–394.
54. Wu A, Ying Z, Gomez-Pinilla F: The interplay between oxidative stress and brain-derived neurotrophic factor modulates the outcome of a saturated fat diet on synaptic plasticity and cognition. *Eur J Neurosci* 2004;19:1699–1707.
55. Erickson KI, Prakash RS, Voss MW, Chaddock L, Heo S, McLaren M, Pence BD, Martin SA, Vieira VJ, Woods JA, McAuley E, Kramer AF: Brain-derived neurotrophic factor is associated with age-related decline in hippocampal volume. *J Neurosci* 2010;30:5368–5375.
56. Caccamo A, Maldonado MA, Bokov AF, Majumder S, Oddo S: CBP gene transfer increases BDNF levels and ameliorates learning and memory deficits in a mouse model of Alzheimer's disease. *Proc Natl Acad Sci USA* 2010;107:22687–22692.
57. Takei S, Morinobu S, Yamamoto S, Fuchikami M, Matsumoto T, Yamawaki S: Enhanced hippocampal BDNF/TrkB signaling in response to fear conditioning in an animal model of posttraumatic stress disorder. *J Psychiatr Res* 2011;45:460–468.
58. Bekinschtein P, Cammarota M, Igaz LM, Bevilaqua LR, Izquierdo I, Medina JH: Persistence of long-term memory storage requires a late protein synthesis- and BDNF-dependent phase in the hippocampus. *Neuron* 2007;53:261–277.
59. Bekinschtein P, Cammarota M, Izquierdo I, Medina JH: BDNF and memory formation and storage. *Neuroscientist* 2008;14: 147–156.
60. Xi G, Zhang X, Zhang L, Sui Y, Hui J, Liu S, Wnag Y, Li L, Zhang Z: Fluoxetine attenuates the inhibitory effect of glucocorticoid hormones on neurogenesis *in vitro* via a two-pore domain potassium channel, TREK-1. *Psychopharmacology (Berl)* 2011;214:747–759.
61. Xu Y, Ku B, Cui L, Li X, Barish PA, Foster TC, Ogle WO: Curcumin reverses impaired hippocampal neurogenesis and increases serotonin receptor 1A mRNA and brain-derived neurotrophic factor expression in chronically stressed rats. *Brain Res* 2007;1162:9–18.
62. Xu Y, Ku BS, Yao HY, Lin YH, Ma X, Zhang YH, Li XJ: Antidepressant effects of curcumin in the forced swim test and olfactory bulbectomy models of depression in rats. *Pharmacol Biochem Behav* 2005;82:200–206.
63. Xia X, Cheng G, Pan Y, Xia ZH, Kong LD: Behavioral, neurochemical and neuroendocrine effects of the ethanolic extract from *Curcuma longa* L. in the mouse forced swimming test. *J Ethnopharmacol* 2007;110:356–363.
64. Kulkarni SK, Bhutani MK, Bishnoi M: Antidepressant activity of curcumin: involvement of serotonin and dopamine system. *Psychopharmacology (Berl)* 2008;201:435–442.
65. Bhutani MK, Bishnoi M, Kulkarni SK: Anti-depressant like effect of curcumin and its combination with piperine in unpredictable chronic stress-induced behavioral, biochemical and neurochemical changes. *Pharmacol Biochem Behav* 2009;92:39–43.
66. Mattson MP, Maudsley S, Martin B: BDNF and 5-HT: a dynamic duo in age-related neuronal plasticity and neurodegenerative disorders. *Trends Neurosci* 2004;27:589–594.
67. Takahashi J, Palmer TD, Gage FH: Retinoic acid and neurotrophins collaborate to regulate neurogenesis in adult-derived neural stem cell cultures. *J Neurobiol* 1999;38:65–81.
68. Banasr M, Hery M, Printemps R, Daszuta A: Serotonin-induced increases in adult cell proliferation and neurogenesis are mediated through different and common 5-HT receptor subtypes in the dentate gyrus and the subventricular zone. *Neuropsychopharmacology* 2004;29:450–460.
69. Yoshii A, Constantine-Paton M: Postsynaptic BDNF-TrkB signaling in synapse maturation, plasticity, and disease. *Dev Neurobiol* 2010;70:304–322.
70. Bramham CR, Messaoudi E: BDNF function in adult synaptic plasticity: the synaptic consolidation hypothesis. *Prog Neurobiol* 2005;76:99–125.
71. Xu Y, Ku B, Tie L, Yao H, Jiang W, Ma X, Li X: Curcumin reverses the effects of chronic stress on behavior, the HPA axis, BDNF expression and phosphorylation of CREB. *Brain Res* 2006;1122:56–64.
72. Wang R, Li YB, Li YH, Xu Y, Wu HL, Li XJ: Curcumin protects against glutamate excitotoxicity in rat cerebral cortical neurons by increasing brain-derived neurotrophic factor level and activating TrkB. *Brain Res* 2008;1210:84–91.
73. Wang R, Li YH, Xu Y, Li YB, Wu HL, Guo H, Zhang JZ, Zhang JJ, Pan XY, Li XJ: Curcumin produces neuroprotective effects via activating brain-derived neurotrophic factor/TrkB-dependent MAPK and PI-3K cascades in rodent cortical neurons. *Prog Neuropsychopharmacol Biol Psychiatry* 2010;34:147–153.
74. Huang Z, Zhong XM, Li ZY, Feng CR, Pan AJ, Mao QQ: Curcumin reverses corticosterone-induced depressive-like behavior and decrease in brain BDNF levels in rats. *Neurosci Lett* 2011;493:145–148.
75. Hurley LL, Akinfiresoye L, Nwulia E, Kamiya A, Kulkarni AA, Tizabi Y: Antidepressant-like effects of curcumin in WKY rat model of depression is associated with an increase in hippocampal BDNF. *Behav Brain Res* 2013;239:27–30.
76. Rinwa P, Kumar A, Garg S: Suppression of neuroinflammatory and apoptotic signaling cascade by curcumin alone and in combination with piperine in rat model of olfactory bulbectomy induced depression. *PLoS One* 2013;8:e61052.